

A 3-Stage Shunt-Feedback Op-Amp having 19.2dB Gain, 54.1dBm OIP3 (2GHz), and 252 OIP3/ P_{DC} ratio

Zach Griffith*, Miguel Urteaga*, Richard Pierson*, Petra Rowell*, Mark Rodwell† and Bobby Brar*

*Teledyne Scientific and Imaging Company

1049 Camino Dos Rios, Thousand Oaks, CA 91360, USA

E-mail: zgriffith@teledyne.com

†Dept. of Electrical and Computer Engineering, University of California, Santa Barbara, CA 93106-9560, USA

Abstract— We report here a 3-stage shunt-feedback configured operational amplifier using simple-Miller compensation demonstrating 19.2dB mid-band S_{21} gain, $P_{DC} = 1020$ mW. At 2GHz operation the amplifier shows 54.1dBm OIP3 and a record high OIP3/ P_{DC} ratio = 252. Through the use of a 350GHz f_{τ} , f_{max} 0.5um InP HBT technology, the loop transmission at low GHz operation provides a large reduction to the closed-loop distortion. The amplifier employs a differential topology, resistive pulldown biasing, large 6nH inductors to act as RF chokes, and a 6-finger ($10\mu\text{m}$ L_e) output stage to increase P_{out} before the onset of waveform clipping. The loop bandwidth is greater than 30GHz, 5.5dB NF, and is unconditionally stable from DC-8.5GHz. The slope-3 breakpoint (S-3BP, where the IM3 spurs are 3dB greater than the expected slope-3 trend) is at $P_{out} = 16.6$ mW/ton. The increases to OIP3/ P_{DC} ratio represent $> 1.7\times$ betterment in state-of-the-art. The circuit contains 24 HBTs and is $0.92\times 0.46\text{-mm}^2$.

Index Terms—Operational-amplifier, Shunt-feedback, Miller compensation, distortion suppression

I. INTRODUCTION

AMPLIFIERS with very low intermodulation distortion are required in radar receivers and multi-carrier communications systems such as cell phone base stations. In simple, reactively-tuned RF amplifiers, the output-referred third-order intermodulation distortion intercept (OIP3) is proportional to the DC current dissipation. In this situation, very low IM3 can be obtained only at the cost of high DC power consumption.

Here we report mm-wave amplifiers having high (greater than 50dBm) third-order intermodulation intercepts despite consuming a relatively low ~ 1000 mW power dissipation P_{DC} . This very large ratio of output-referred third-order-intercept power to DC power consumption, $P_{OIP3}/P_{DC} > 250$, is obtained through the use of strong global negative feedback using circuit techniques similar to classic operational amplifiers [1]. We explicitly distinguish this work from that of other mm-, microwave feedback amplifiers using a feedback resistor $R_f = Z_o(1 - A_v)$ [2] which provides a matched Z_o input impedance; such amplifiers have less than unity feedback magnitude. In marked contrast, low amplifier distortion is obtained here using strong global negative feedback; in other words, a mm-wave operational amplifier.

Obtaining high OIP3 at low GHz operation requires novel designs and detailed attention to residual sources of distortion. Because > 30 GHz loop bandwidths are required, stability is critically sensitive to layout and interconnect parasitics. Frequency compensation limits the degree of reduction of output-stage distortion and increases the distortion associated with stages nearer the input. Difficulties arise from inadvertent non-linear loading of the feedback network by transistor junction capacitances. Challenges include the control of input and output impedances, and the sensitivity of the loop bandwidth – i.e. phase margin to generator and load impedances.

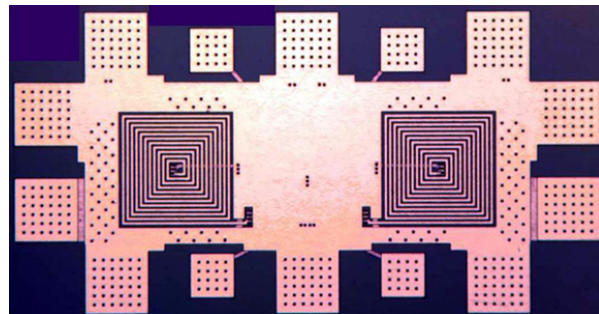


Fig. 1. IC micrograph of the 3-stage simple-Miller compensated op-amp. Die area, $0.92\times 0.46\text{-mm}^2$.

Manufacturable InP heterojunction bipolar transistor (HBT) IC technologies offer 350GHz cutoff frequencies [3], [4] and breakdown voltages BV_{ceo} near 5V. With appropriate design, stable feedback loops with > 30 GHz bandwidth are feasible in this technology, providing strong feedback at low GHz operation for strong distortion suppression.

Prior to the results reported here, it has been reported in [5] an op-amp utilizing strong feedback which demonstrated 51.4dBm OIP3 at 2GHz operation ($OIP3/P_{DC} = 144$) and the S-3BP was at $P_{out} = 5.6$ mW per tone (49.9dBm OIP3). We report here a 3-stage shunt-feedback amplifier designed to demonstrate higher OIP3, maintain high OIP3 at higher P_{out} , while keeping P_{DC} under 1W. This amplifier demonstrates 19.2dB mid-band S_{21} gain, > 30 GHz loop-bandwidth, 5.5dB NF, and is unconditionally stable ($k' > 1$) from DC-8.5GHz, with 1020mW P_{DC} . At $f_{1,2} = 1.80, 1.90$ GHz, OIP3 is 54.1 dBm, and S-3BP is at $P_{out} = 16.6$ mW per tone (52.6dBm OIP3). Compared to [5], the increases to OIP3 and OIP3/ P_{DC} ratio represent $> 1.7\times$ betterment in state-of-the-art for high linearity, high bandwidth amplifiers employing strong feedback.

II. THEORY

An amplifier (fig. 2a) having open-loop distortion V_e produces a closed-loop output of $V_{out} = A_{CL}V_{in} + (A_{CL}/A_{OL})V_e$, where $A_{CL} \cong 1/H$ is the closed-loop gain. Distortion is reduced by the ratio (A_{CL}/A_{OL}) of the closed-loop to open-loop gain. In a two-stage design (fig. 2b), each stage first produces open-loop intermodulation distortions (V_{e1}, V_{e2}) determined by the magnitude of the stage output signals (V_{out1}, V_{out2}) and third-order intercepts ($V_{OIP3,1}, V_{OIP3,2}$) through the relationships $V_{e2} = V_{out2}^3/V_{OIP3,2}^2$ and $V_{e1} = V_{out1}^3/V_{OIP3,1}^2 = (V_{out}/A_{v,2})^3/V_{OIP3,1}^2$. The closed-loop output is then $V_{out} = A_{CL}V_{in} + (A_{CL}/A_1)V_{e1} + (A_{CL}/A_1A_2)V_{e2}$. The amplifier must be frequency compensated for stability, $A_1A_2H = f_{unity}/jf$, by making either A_1 or A_2 vary as $1/jf$. In the first case, if $A_1 \propto 1/jf$, the closed-loop distortion terms $(A_{CL}/A_1)V_{e1}$ and $(A_{CL}/A_1A_2)V_{e2}$ increase at high frequencies. In the second case, if $A_2 \propto 1/jf$ for constant

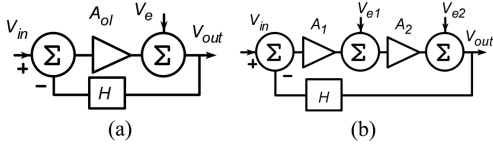


Fig. 2. Error (distortion) analysis of feedback amplifiers: (a) single-stage and (b) multi-stage feedback amplifier with global feedback.

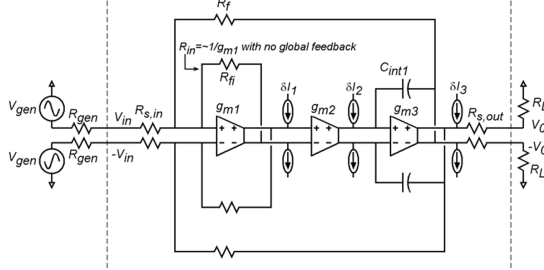


Fig. 3. Current-mode operational amplifier in simple-Miller form using HBT differential \$g_m\$ blocks. Amplifier distortion currents are illustrated.

V_{out2} , V_{out1} varies as jf and V_{e1} consequently varies as $(jf)^3$ [6]. Distortion in either case increases with higher frequency operation.

The amplifiers in this work are in the current-mode form and use simple-Miller compensation (fig. 3). The blocks g_{m1}, g_{m2} are degenerated HBT differential pairs; the output stage (g_{m3}) is a differential pair having emitter-follower input buffers. When brought together, the simple-Miller amplifier consists of the g_{m2}, g_{m3} Miller integrators, and a transimpedance input stage (g_{m1}).

We now extend the earlier distortion analysis. Assume that $R_{s,out} \ll R_L$. With a two-tone ($f_1 = f_s + \varepsilon, f_2 = f_s - \varepsilon$) output signal, where each tone is of root-mean-square (RMS) amplitude V_{out} , the RMS currents of (g_{m1}, g_{m2}, g_{m3}) at f_1 and at f_2 are $I_{out3} \cong (1/R_L + j2\pi f_s C_{int1})V_{out}$, $I_{out2} \cong j2\pi f_s C_{int1}V_{out}$, and $I_{out1} \cong j2\pi f_s (C_{int1}/g_{m2}R_{fi})V_{out}$. Because of the $I_c = I_s \exp(qV_{be}/\eta kT)$ HBT characteristics, each stage produces distortion currents ($\delta I_1, \delta I_2, \delta I_3$) at $(2f_1 - f_2, 2f_2 - f_1)$ of RMS amplitudes $\delta I_1 = I_{out1}^3/I_{OIP3,1}^2$, $\delta I_2 = I_{out2}^3/I_{OIP3,2}^2$, and $\delta I_3 = I_{out3}^3/I_{OIP3,3}^2$ - where each stage's output-referred IP3 is simply its DC bias current. The amplifier's closed-loop gain is $A_{CL} = V_{out}/V_{gen} = R_f/(R_{gen} + R_{s,in})$, while $S_{21} \cong 2R_f/(Z_o + R_{s,in})$. The closed-loop output voltage contains frequency components at $(2f_1 - f_2, 2f_2 - f_1)$, each of RMS amplitude δV_{out} , where

$$\delta V_{out} = \left(\frac{\delta I_3}{g_{m3}}\right) \left(\frac{jf}{f_{unity1-2-3}}\right) + \left(\frac{\delta I_2}{g_{m2}}\right) \left(\frac{R_f}{R_{fi}}\right) + \left(\frac{\delta I_1}{g_{m1}}\right) \left(\frac{R_f}{R_{s,in} + R_{gen}} + \frac{R_f}{R_{fi}}\right) \quad (1)$$

where $f_{unity1-2-3} \cong (g_{m2}R_{fi}/C_{int1}R_f)$ is the unity-gain frequency of the feedback loop transmission, where $T \sim f_{unity1-2-3}/jf$. We can now see the importance of using a 350 GHz f_τ, f_{max} HBT technology, as $f_{unity1-2-3} \sim 30$ -40 GHz are feasible, and at $f_s \sim 2$ GHz, considerable reduction in the output stage distortion is therefore feasible. Note: compensation strongly impacts distortion, as the 2^{nd} -stage output current is $I_{out2} \cong j2\pi f_s C_{int1}V_{out}$ and becomes large at high frequencies. Appropriate sizing of C_{int1} must be considered.

The effect of non-linear capacitive loading of the feedback network is of paramount importance. In a simple series-shunt feedback amp (fig. 4a), low distortion is not obtained even with strong feedback. Considering separately (fig. 4b) the effect of the input (A_1) and subsequent (A_2) stages, in the limit of large loop gain

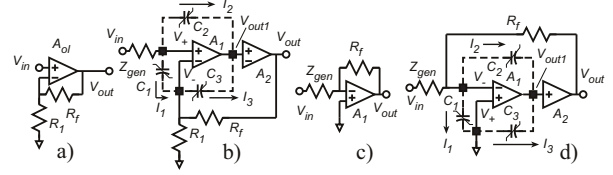


Fig. 4. Distortion from some non-linear impedances is not reduced by feedback. An elementary voltage-sum amplifier (a), when loaded by the non-linear input-stage capacitances (b) suffers from non-linear loading of the feedback network. An elementary current-sum amplifier (c), if constructed in multi-stage form (d) avoids these effects.

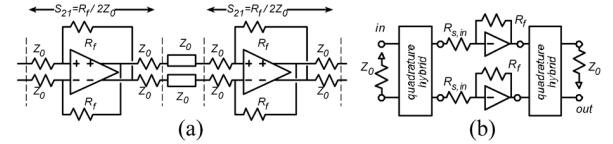


Fig. 5. Managing input and output impedances by (a) transmission-line series termination and (b) through the balanced amplifier configuration.

$T = A_1 A_2 R_1 / (R_f + R_1) \rightarrow \infty$, the differential input signal ($V^+ - V^-$) is driven to zero, driving to zero the current I_1 associated with the non-linear input capacitance C_1 . The voltages ($V^+ - V_{out1}$) and ($V^- - V_{out1}$) are driven *not to zero* but to $V_{in}(1 - A_{CL}/A_2)$ as $T \rightarrow \infty$; hence the currents (I_1, I_2) flowing through the input stage's non-linear base-collector capacitances (C_2, C_3) also remain nonzero. These currents (I_1, I_2) produce voltage drops across the feedback network impedances (Z_{gen}, R_1, R_f), producing closed-loop distortion even in the limit $T \rightarrow \infty$. The shunt-shunt feedback amplifier (fig. 4c,d) avoids this limitation - in the limit $A_2 \rightarrow \infty$, the voltages ($V^+ - V^-$), ($V^+ - V_{out1}$), and ($V^- - V_{out1}$) are all driven to zero, forcing (I_1, I_2, I_3) $\rightarrow 0$. Our designs therefore use the shunt-shunt configuration.

The generator and load impedances will change the loop transmission T and unfavorable values may cause oscillation. We must clearly distinguish between stability in a 50 Ω system and stability with arbitrary generator and load (unconditional stability) impedances. Even before applying global feedback, the *open-loop* output impedance is low because of the local feedback through C_1 ; hence even ~ 5 -10 Ω series padding, $R_{s,out}$, provides a large range of *load* impedances for which the loop is stable. The transimpedance input stage (g_{m1}) provides an *open-loop* input impedance $R_{in,open-loop} \cong 1/g_{m1}$; provided that $\|Z_{gen} + R_{s,in}\| < 1/g_{m1}$, T is then only weakly dependent upon Z_{gen} . This provides a wide range of *generator* impedances for which the loop is stable. Additionally, because the loop bandwidth is ~ 20 -40 GHz while $f_s \sim 2$ GHz, unconditional stability can be obtained by isolating at high frequencies the feedback amplifier from the external load using frequency-selective networks - as is standard in audio power amplifiers.

Finally, note that the shunt-shunt feedback forces $Z_{in} \rightarrow R_{s,in}$ and $Z_{out} \rightarrow 0 \Omega$. If impaired noise figure and output power can be accepted, matched line interfaces can be provided by series padding (fig. 5a). However, if highest OIP3 and lowest noise figure are required, one must set $R_{s,in} \ll Z_o$ and $R_{s,out} \ll Z_o$, which leads to poor S_{11} and S_{22} . In this case, a balanced amplifier configuration (fig. 5b) will provide low return losses over many octaves of bandwidth even with minimal or zero series input and output padding. Alternatively, if small padding is acceptable for $R_{s,in}$ and $R_{s,out}$, a 2:1 or 4:1 balun-transformer can be used at the input and output to transform the padding resistance to Z_o .

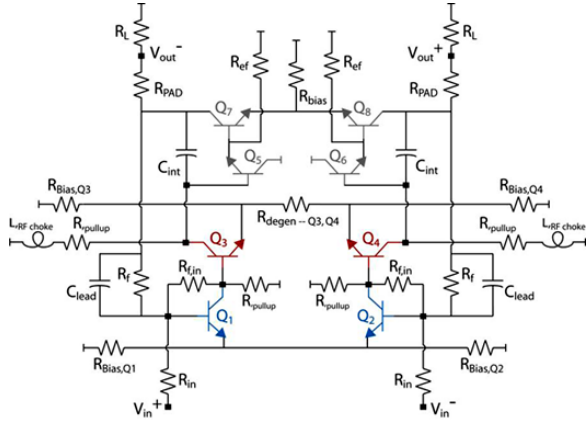


Fig. 6. Circuit schematic and floorplan of the 3-stage, shunt-feedback, simple-Miller-compensated op-amp.

III. DESIGN

Our amplifier is a differential 3-stage op-amp using a simple resistive shunt feedback network. To ensure the network is dominantly real across the amplifier loop bandwidth, the length of the feedback path is kept to $65 \mu\text{m}$ to avoid unintentional reactive loading by the interconnect. This short length is possible with the symmetric, folded floorplan used for circuit layout (figure 6). The amplifier employs an input transimpedance stage to reduce the loop transmission dependence on the generator source impedance. The local-stage bias currents are chosen so that the output referred distortion of no one stage greatly exceeds the others. The loop bandwidth is set by the stage-2 gain and integration capacitance, $g_{m,2}/C_{int} \cong (C_{int}(R_{ex,Q3-Q4}/2))^{-1}$. A small C_{lead} capacitance is used in parallel with the feedback resistor to improve the amplifier phase margin when the loop bandwidth is near the gain-bandwidth product. To improve the output return-loss and amplifier stability, a small 5Ω padding resistance is used. For the amplifiers presented, $R_f = 300 \Omega$, $R_{f,in} = 350 \Omega$, and $R_{in} = 6 \Omega$.

The bias currents are set using a single voltage supply $V_{EE} = -4.45\text{V}$ and pulldown resistors for each stage ($I_{EE} = 229.4\text{mA}$). The input-voltage is $V_{in} = -1.85\text{V}$ ($I_{in} = 10.0\text{mA}$). The output-voltage is $V_{out} = 0.0\text{V}$ ($I_{out} = 131.2\text{mA}$); the collector-emitter voltage V_{CE} of the output stage is 2.8V to center the quiescent bias so that the waveform compresses evenly between HBT saturation and cut-off operating limits. Because the bias current of stage-2 is large, $R_{pullup,2}$ must be small to correctly set the stage-3 voltage at $Q_{5,6}$. To avoid a larger local distortion current from $Q_{3,4}$ by having only small $R_{pullup,2}$ load the collector of stage-2 (in parallel with stage-3 input), and to increase stage-2 gain for higher A_{ol} and loop transmission, a large 6nH inductor is placed in-series to act as an RF choke ($Z = R_{pullup,2} + j\omega L$) since complimentary devices are not available.

The circuit was formed using a $0.5\mu\text{m}$ HBT technology. A 3-metal layer wiring is formed using low-loss, thin-film dielectric (Benzocyclobutene, $\epsilon_r = 2.7$) having $1\mu\text{m}$ inter-metal spacing. Inverted thin-film microstrip wiring ($3\mu\text{m}$ thick) is used for the circuit interconnect. Figure 1 shows an IC micrograph of the fabricated 3-stage, shunt-feedback op-amp; its size is $0.92 \times 0.46 \mu\text{m}^2$.

IV. MEASUREMENT SETUP

4-port RF measurements of the circuit were performed from 100MHz - 50GHz using an Agilent PNA-X N5245 network analyzer after SOLT calibration. Figure 7 shows the configuration for the two-tone and intermodulation distortion measurement system, where an Agilent 4440A PSA spectrum analyzer is used. Measurement

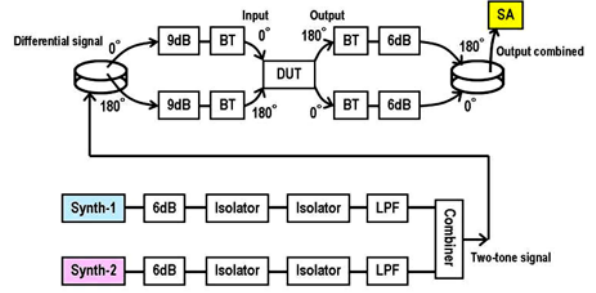


Fig. 7. Test-bench for differential two-tone power and intermodulation distortion measurements.

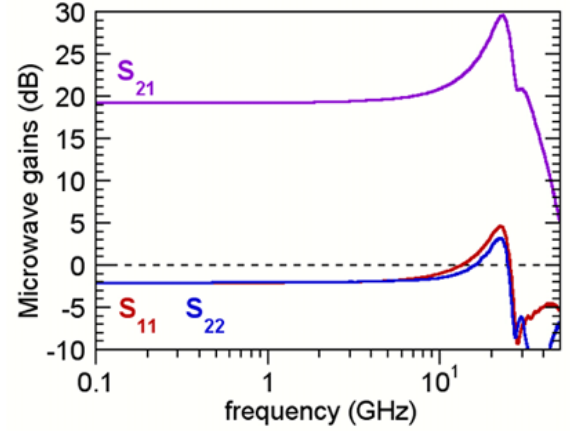


Fig. 8. Measured differential S-parameters of the 3-stage, shunt-feedback op-amp. $C_{int} = 200\text{fF}$, $R_{ex,Q3-Q4} = 50\Omega/2$.

of a differential thru-line shows 56 dBm OIP3 of residual system distortion.

Noise figure measurements are performed using an Agilent 3466 noise source and 8971C noise test set jointly with the differential 180° hybrid-rings from the two-tone measurement setup. Once the noise source and test-set are calibrated, circuit measurements are performed. The noise figure of the op-amp is extracted through the use of Friis' equation [7] so we may deembed the cascaded stages of the input and output (effective 2-port) hybrid rings.

V. CIRCUIT RESULTS

Differential S-parameters of the 3-stage, shunt-feedback op-amp are shown in figure 8. The mid-band S_{21} gain is 19.2dB and $P_{DC} = 1020\text{mW}$. From the Rollett stability factor 'K', the amplifier is unconditionally stability from DC- 8.5GHz . The loop bandwidth was designed to be 31GHz , set by $C_{int} = 200\text{fF}$ and $R_{ex,Q3-Q4} = 50\Omega/2$. Unlike the simulated performance for the amplifier, at frequencies past 13GHz , strong S_{21} gain peaking is observed and S_{11} , S_{22} are $> 0\text{dB}$. Upon revisiting the amplifier simulation and using data from similar parts (where the size of the output stage HBTs is varied), we conclude that the emitter interconnect of the output stage contains series inductance as it forms the differential AC ground, greatly reducing the phase margin of the feedback amplifier. By using an additional AC ground strap between the differential output stage devices, simulation shows (fig. 9) the effects of the series inductance become negligible, the gain peaking in S_{21} is reduced from 12dB to 6dB , S_{11} and S_{22} become $< 0\text{dB}$, and there is no change to the amplifier OIP3.

Differential two-tone power and third-order intermodulation (IM3) distortion measurements were performed. The expected P_{in}

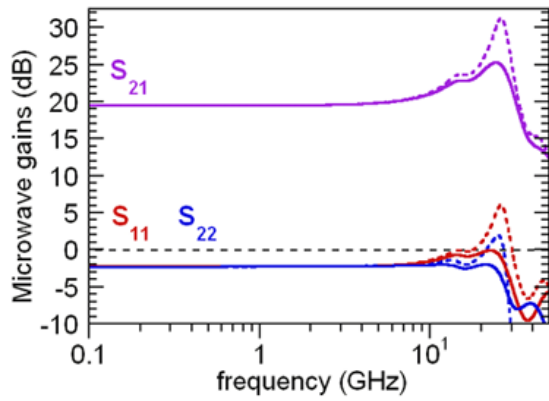
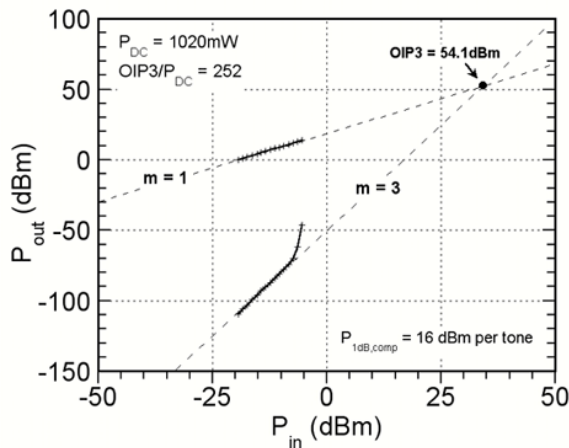
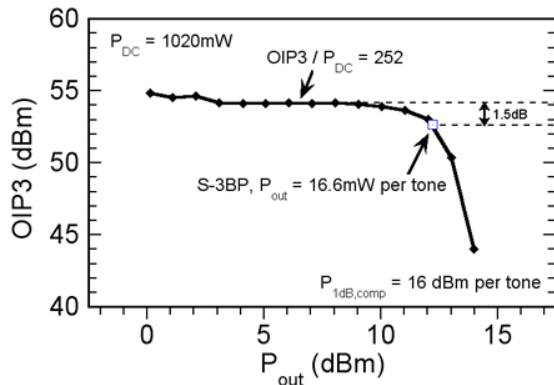


Fig. 9. Simulated differential S-parameters of the 3-stage, shunt-feedback op-amp showing how the additional emitter AC ground strap (solid line with the strap, dashed without) impacts the amplifier RF performance.



(a) P_{out} and P_{IM3} versus P_{in} .



(b) Variation of OIP3 for increasing values of P_{out}

Fig. 10. Two-tone and IM3 power measurements, where the amplifier OIP3 is extrapolated. $f_{1,2} = 1.80, 1.90\text{GHz}$, $f_{IM3} = 1.7, 2.0\text{GHz}$

versus P_{out} trends for the fundamentals and IM3 products are clearly observed and OIP3 is extrapolated, plotted in figure 10(a). At $f_{1,2} = 1.8, 1.9\text{GHz}$ operation, the amplifier demonstrated 54.1dBm OIP3 and OIP3/ P_{DC} ratio of 252. The variation of amplifier OIP3 with increasing signal output power is shown in figure 10(b). The slope-3 breakpoint (S-3BP, where the IM3 spurs are 3dB greater than the expected slope-3 trend) is at $P_{out} = 16.6\text{mW/tonne}$, where OIP3 = 52.6dBm. For $P_{out} = 20\text{mW}$ per tone, the amplifier OIP3 is still greater than 50dBm, and the P_{1dB} compression is 16dBm per tone.

ACKNOWLEDGMENT

This work was supported under the DARPA FLARE program by SPAWAR System Center. The views, opinions, and/or findings contained in this article are those of the authors and should not be interpreted as representing the official views or policies, either expressed or implied, of the Defense Advanced Projects Agency or the Department of Defense. Special thanks to Program Manager Dr. Sanjay Raman, and Dr. Richard Eden for their contributions and support.

REFERENCES

- [1] J.E. Solomon, *IEEE Journal of Solid-State Circuits*, Vol. SC-9, No. 6. Also at <http://www.national.com/an/AN/AN-A.pdf>
- [2] M. Rodwell, J. Jensen, W. Stanchina, R. Metzger, D. Rensch, M. Pierce, T. Kargodorian, Y. Allen, "33GHz Monolithic Cascode AlInAs/GaNAs Heterojunction Bipolar Transistor Feedback Amplifier", *IEEE Journal of Solid-State Circuits*, Vol. 26, No. 10, pp. 1378-1382, October 1991.
- [3] M. Urteaga, R. Pierson, P. Rowell, M. Choe, D. Mensa, B. Brar, "Advanced InP DHB T Process for High Speed LSI Circuits", *Conf. Proc. Indium Phosphide and Related Circuits*, Versailles, France, May 25-29, 2008.
- [4] A. Gutierrez-Aitken, C. Monier, P. Chang, E. Kaneshiro, D. Scott, B. Chan, M. D'Amore, S. Lin, B. Oyama, K. Sato, A. Cavus, A. Oki, "Advanced InP HBT Technology at Northrup Grumman Aerospace Systems", *Proc. IEEE Compound Semiconductor IC Symposium*, Greensboro, NC, October 11-14, 2009.
- [5] Z. Griffith, M. Urteaga, M. Rodwell, "mm-Wave Op-Amps employing simple-Miller Compensation, with OIP3/ P_{DC} ratio of 211 (10dB NF) and 144 (6.0dB NF) at 2GHz", *Proc. IEEE Compound Semiconductor IC Symposium*, Monterey, CA, October 12-15, 2008.
- [6] E. Chery, *IEEE Transactions on Acoustics, Speech, and Signal Process.*, Vol. 29, Iss. 2, Apr. 1981, pp. 137-146.
- [7] A. van der Ziel, *Noise: Sources, Characterization, Measurement*. Englewood Cliffs, NJ, Prentice-Hall, 1970.